# Nuclear export inhibitor Selinexor targeting XPO1 enhances coronavirus replication

Masmudur M. Rahman[1], Bereket Estifanos[1 2], Honor L. Glenn[1], Karen Kibler[1], Yize Li[1 3], Bertram Jacobs[1 3], Grant McFadden[1 3], Brenda G. Hogue[1 3]

1 Center for Immunotherapy, Vaccines, and Virotherapy, Biodesign Institute, Arizona State University, Tempe, AZ 85287, USA.

2 School of Life Sciences Microbiology Graduate Program, Arizona State University, Tempe, AZ 85287, USA

3 School of Life Sciences, Arizona State University, Tempe, AZ 85287, USA

Corresponding authors:

Masmudur M. Rahman: masmudur.rahman@asu.edu

Brenda G. Hogue: brenda.hogue@asu.edu

**Abstract**

Nucleocytoplasmic transport of proteins using XPO1 (exportin 1) plays a vital role in cell proliferation and survival. Many viruses also exploit this pathway to promote infection and replication. Thus, inhibiting XPO1-mediated nuclear export with selective inhibitors activates multiple antiviral and anti-inflammatory pathways. The XPO1 inhibitor, Selinexor, is an FDA-approved anticancer drug predicted to have antiviral function against many viruses, including SARS-CoV-2. Unexpectedly, we observed that pretreatment of cultured human cells with Selinexor actually enhanced protein expression and replication of coronaviruses, including SARS-CoV-2. Knockdown of cellular XPO1 protein expression significantly enhanced the replication of coronaviruses in human cells. We further demonstrate that Selinexor treatment reduced the formation of unique cytoplasmic antiviral granules that include RNA helicase DHX9 in the virus-infected cells. These results, for the first time, show that the anti-cancer drug Selinexor enhances the replication of coronaviruses in human cells *in vitro* and thus should be further explored *in vivo* for the potential impact on the dual use for anticancer and antiviral therapy.

43 **Introduction**

44 The nucleocytoplasmic transport of proteins and other molecules is a highly regulated cellular
45 process. Many nuclear export (called exportins) and import (called importins) proteins are
46 involved in this process by exploiting nuclear pore complexes that form proteinaceous channels
47 in the nuclear envelope (1, 2). Exportin 1 (XPO1), also known as CRM1 (chromosome region
48 maintenance 1), is one of the major nuclear export proteins, transporting hundreds of cellular
49 cargo proteins involved in diverse cellular processes such as transcription, translation, cellular
50 growth, differentiation, and mediating inflammatory responses that include antiviral pathways (3,
51 4). Thus, direct inhibition of XPO1 function has been explored as a potential antiviral and
52 anticancer therapeutic target (5-8). Various natural or chemically synthesized small molecules
53 that bind to XPO1 and block the export of XPO1 cargo proteins from the nucleus to the cytoplasm
54 have been developed (9, 10). Collectively these molecules are known as selective inhibitors of
55 nuclear export (SINEs). SINEs have been shown to have anticancer activity against diverse types
56 of human cancers and at least one modified drug version with increased safety profile, called
57 Selinexor, has been approved by the FDA for treating multiple myeloma and diffuse large B-cell
58 lymphoma (11, 12). SINEs are also reported in the literature to have antiviral activity against RNA
59 viruses like influenza and respiratory syncytial virus (RSV) that causes respiratory infections due
60 to the blocking of key cellular processes and virus-mediated hijacking of the nucleocytoplasmic
61 transport process (6, 13, 14).

62 Coronaviruses are enveloped, positive-sense RNA viruses that are known to infect humans and
63 animals. At least seven coronaviruses are known to infect humans. Coronaviruses 229E, NL63,
64 OC43, and HKU1 infect people around the world to cause the common cold (15). Other
65 coronaviruses, MERS-CoV, SARS-CoV, and SARS-CoV-2, are responsible for major disease
66 outbreaks and cause high mortality (16). SARS-CoV-2, which causes COVID-19 killed millions
67 globally due to the ongoing pandemic (https://coronavirus.jhu.edu/map.html). In nature, bats are

68 known to be primary reservoirs of many coronaviruses, from where viruses spill over to
69 intermediate animals such as palm civet, pangolins, rodents, camels, pigs, cattle where viruses
70 evolve and then spillover to humans, causing mild to severe disease (17, 18). The rapid
71 emergence of different variants of SARS-CoV-2 indicates that the viral genome acquire multiple
72 mutations during replication (19, 20). In this context, it is crucial to study the host factors and
73 compounds that can enhance or reduce replication of SARS-CoV-2 (21-23). It is possible that
74 factors which enhance virus replication can also enhance mutational rates in the viral genome.

75 Recently, it was reported that the XPO1 inhibitor Selinexor enhanced the nuclear localization of
76 ACE-2 protein, the primary receptor for SARS-CoV-2 (24). Selinexor treatment thus reduced virus
77 entry and infection *in vitro* and the viral load in the lungs in a COVID-19 ferret model (24). In
78 addition, Selinexor treatment downregulated the expression of pro-inflammatory cytokines, which
79 are associated with cytokine storm observed in COVID-19 patients (24, 25).

80 We previously reported that XPO1 inhibitors, including leptomycin B (LMB) and Selinexor,
81 enhanced the replication of oncolytic myxoma virus (MYXV), a member of the leporipoxvirus
82 genus of *poxviridae,* in diverse types of cultured human cancer cells where intrinsic cellular
83 pathways restrict virus replication (26). In addition, Selinexor treatment reduced the formation of
84 cytoplasmic DHX9 antiviral granules, which are involved in lowering MYXV late protein synthesis
85 and replication. Selinexor also enhanced the nuclear localization of DHX9 and, as predicted,
86 blocked the XPO1-mediated export of DHX9 nuclear transport (26). These findings led us to
87 investigate further the role of Selinexor-mediated inhibition of XPO1 nuclear export pathway on
88 other viruses.

89 Here, we show that Selinexor treatment unexpectedly enhances the *in vitro* replication of
90 coronaviruses, including SARS-CoV-2, which replicate in the cytoplasm of infected cells. This
91 enhanced replication of the virus by Selinexor was confirmed in murine and human cell lines.
92 Furthermore, the targeted knockdown of XPO1 using siRNA also enhanced coronavirus

93 replication, suggesting the pro-coronavirus drug action is indeed related to the expected nuclear
94 export pathway target. Coronavirus infection in human cells results in the unique localization of
95 RNA helicase DHX9 in the cytoplasm, which is blocked with Selinexor treatment. The observation
96 that Selinexor treatment exacerbates coronavirus infection of human cells in vitro should serve
97 as a cautionary note to carefully track SARS-CoV-2 infections in cancer patients when treated
98 with the drug.

99 **Results**

100 **Nuclear export inhibitor Selinexor enhances gene expression and replication of**
101 **coronavirus in murine L2 cells.**

102 Murine L2 cells are naturally infected by the mouse hepatitis virus (MHV). We first monitored and
103 measured the viability of L2 cells in response to treatment with different concentrations of
104 Selinexor (Fig 1A). L2 cell viability was reduced only after treatment with a Selinexor concentration
105 of 5μM or above but had minimal or no effect with a concentration of 1 μM or less. To test the
106 effect of Selinexor on MHV replication, L2 cells were first pretreated with different concentrations
107 of Selinexor for one hour and infected with a GFP-expressing MHV A59 (rA59/$S_{MHV-2}$-EGFP) to
108 monitor the level of GFP expression in the infected cells (27-29). Infection with this MHV exhibits
109 reduced cell fusion since the virus expresses a less fusogenic form of the spike protein and thus
110 allowed counting the number of GFP positive cells. We observed the enhanced GFP expression
111 in L2 cells pretreated with Selinexor between 10 and 0.01 μM concentration (Fig 1B). We
112 confirmed the enhanced expression of GFP by counting the number of GFP-positive cells (Fig
113 1C). To assess the number of viruses produced in the presence of Selinexor, L2 cells were treated
114 with different concentration of Selinexor and infected with another GFP expressing MHV A59
115 (MHVE-GFP) that expresses a highly fusogenic form of spike and readily forms plaques. After
116 24h post infection, the infected cells and supernatant were collected to titer the progeny virus
117 formation by plaque assay. Virus titration results show a significantly enhanced number of viruses

118 in the cells pretreated with Selinexor between 1 and 10 μM concentration (Fig 1D). These results
119 confirm that Selinexor enhances MHV replication and progeny virus formation in naturally
120 permissive L2 cells.

121 **Selinexor enhances gene expression and replication of coronavirus in human cells.**

122 To further confirm the effects of Selinexor on MHV replication, we used human cell lines
123 expressing MHV receptor (MHVR) carcinoembryonic antigen-related cell adhesion molecule 1
124 (CECAM1), HeLa-MHVR (human HeLa cell line expressing MHVR) (30) and A549-
125 CECAM/MHVR (human A549 cell line expressing MHVR) (31). Both cell lines were first treated
126 with different concentrations of Selinexor to test the cell viability (Fig 2A and 3A). Unlike L2 cells,
127 Selinexor concentrations above 1uM significantly reduced viability of the human cells. However,
128 with a concentration of less than 0.1uM, we observed minimal or no reduction in the cell viability.
129 To assess whether Selinexor enhances MHV replication in the human cell lines, both were
130 pretreated with different concentrations of Selinexor for one hour and infected with a GFP-
131 expressing MHV, rA59/$S_{MHV-2}$-EGFP to monitor GFP expression in the infected cells. We
132 observed enhanced GFP expression when pretreated with Selinexor at a concentration of 0.01
133 μM or more (Fig 2B). Enhanced GFP expression was further confirmed by counting the number
134 of GFP-positive cells (Fig 2C and 3B). To assess the amount of virus produced in the presence
135 of Selinexor, HeLa-MHVR (Fig 2D) and A549-MHVR (Fig 3C) cells were treated with different
136 concentration of the drug and infected with MHVE-GFP. Again, like L2 cells, we observed
137 significantly enhanced virus production in both the human cell lines when pretreated with
138 Selinexor between 1 and 0.01 μM concentration (Fig 2D and 3C).

139 **XPO1 knockdown enhances coronavirus gene expression and replication**

140 Since inhibition of the XPO1-mediated nuclear export pathway using Selinexor enhanced
141 coronavirus replication, we further extended this observation by direct knockdown of XPO1 using
142 siRNA. After transfection of XPO1 siRNA or a non-targeting control siRNA (NT-siRNA) in A549-
143 MHVR cells, the cells were infected with different MOIs of the GFP expressing MHV, rA59/$S_{MHV-}$

144 $_2$-EGFP or MHVE-GFP. An increase in GFP-expressing cells was observed only in the XPO1
145 knockdown cells (Fig 4A). Furthermore, the enhanced number of GFP-positive cells in the XPO1
146 knockdown cells compared to controls was confirmed by counting the number of GFP-positive
147 cells (Fig 4C). The level of XPO1 protein knockdown using siRNA was confirmed by western blot
148 analysis (Fig 4B). To quantify the number of progeny virions in the infected cells and supernatant,
149 the cells were infected with MHVE-GFP and samples were collected 24h post-infection. Virus
150 titration shows that significantly increased virus production in the XPO1 knockdown cells
151 compared to the NT-siRNA control or cells infected with the virus alone (Fig 4D), indicating that
152 the effect of Selinexor is mediated by XPO1.

153 **Selinexor enhances gene expression and replication of SARS-CoV-2.**

154 We next tested whether Selinexor enhances the replication of SARS-CoV-2 in human cells. We
155 used a human A549 cell line expressing the ACE2 receptor ($A549^{ACE2}$) and a SARS-CoV-2 virus
156 expressing GFP (SARS-CoV-2-GFP) (32). The $A549^{ACE2}$ cell line showed a similar level of
157 sensitivity to different concentrations of Selinexor like A549-MHVR (data not shown). To assess
158 whether Selinexor enhances SARS-CoV-2 gene expression and replication, $A549^{ACE2}$ cells were
159 first pretreated with 0.01μM of Selinexor for one hour and infected with SARS-CoV-2-GFP. After
160 24h, cells were collected and fixed for counting the number of GFP-positive cells. A significantly
161 increased number of GFP-positive cells were observed in the treated infected cells compared to
162 the untreated cells (Fig 5A). In another experiment, the infected cells and supernatant were
163 collected to titer the progeny virus formation. Virus titration showed significantly increased virus
164 production in the treated cells (Fig 5B). These results indicate that, like MHV, Selinexor enhances
165 the replication of SARS-CoV-2 in human cells.

166 **Selinexor treatment inhibited the unique cytoplasmic localization of DHX9 in the**
167 **coronavirus-infected human cells to enhance viral gene expression.**

168 RNA helicase DHX9 forms cytoplasmic antiviral granules to restrict the cytoplasmic replication of
169 poxviruses such as MYXV and orthopoxvirus vaccinia virus (VACV) in human cells (33). We

170 tested whether the nuclear localization of DHX9 is changed during the cytoplasmic replication of
171 coronavirus. In uninfected A549-MHVR, as expected, DHX9 is mainly localized in the nucleus
172 (Fig 6A, top panels). However, when infected with MHV, DHX9 was detected also in the cytoplasm
173 of infected cells, mainly in the perinuclear region (Fig 6A, middle panels). We then tested whether
174 Selinexor treatment had any effect on the cytoplasmic localization of DHX9 during coronavirus
175 infection. Selinexor treatment completely blocked the cytoplasmic localization of DHX9 in the
176 coronavirus-infected cells (Fig 6A, bottom panels). Based on these observations, in a separate
177 experiment we infected A549-MHVR cells with MHV and tittered progeny virus in the supernatant
178 and cells separately in the presence or absence of Selinexor. Virus titration demonstrated that
179 cells treated with Selinexor have more virus in the cells than the supernatant (Fig 6B). These
180 results suggest that the newly produced viruses from the Selinexor treatment are mainly localized
181 within the infected cells.

182 **Discussion**

183 The nucleocytoplasmic transport process mediated by XPO1 plays a vital role in the export of
184 hundreds of proteins from the nucleus. The proteins are involved in diverse cellular processes
185 such as cell proliferation, cell cycle progression, and apoptosis (1, 5). Thus, the XPO1-mediated
186 export pathway is targeted by viruses at various stages of their lifecycle to regulate cellular
187 proteins and the appropriate localization of viral proteins (6, 34). Apart from viruses, this nuclear
188 export pathway is also crucial for anticancer therapy due to the export of tumor suppressor
189 proteins by XPO1 to the cytoplasm (7, 10). Therefore, XPO1 inhibitors are developed as potential
190 antiviral and anticancer agents. In the nucleus, XPO1 binds to cargo proteins in the presence of
191 RanGTP via an NES (nuclear export sequence) composed of a cluster of leucine (L)-rich or
192 hydrophobic amino acids. After transiting to the cytoplasm, the hydrolysis of RanGTP by RanGAP
193 (a GTPase) disassembles the trimeric complex, and XPO1 reenters the nucleus. The cysteine
194 residue within the hydrophobic NES-binding region at position 528 is the prime target for most

195 XPO1 inhibitors, including leptomycin B (LMB). LMB isolated from Streptomyces was the first
196 specific inhibitor of XPO1 (35). However, the clinical development was discontinued due to severe
197 cell toxicity (36). The irreversible binding of LMB with CRM1 caused long-term inhibition of CRM1-
198 mediated nuclear export, and possible other off-target activity resulting in cellular toxicity (36).
199 Synthetic derivatives of LMB with less toxicity due to the reversible binding with CRM1 have been
200 clinically tested in human. The FDA has approved one such XPO1/CRM1 inhibitor called
201 Selinexor for treating hematological cancers (11). XPO1 inhibitors have shown antiviral activity
202 against many viruses, such as influenza, RSV, and recently SARS-CoV-2 (13, 34, 37, 38).

203 We recently reported that, unlike RNA viruses, LMB or Selinexor enhances the replication of
204 oncolytic MYXV, a leporipoxvirus developed for cancer treatment (26). In human cancer cells,
205 Selinexor enhanced MYXV replication only at a low concentration that had minimal or no toxicity
206 to the cells. However, a higher concentration of Selinexor that caused cellular toxicity also
207 reduced virus replication. Based on our observation that Selinexor can enhance cytoplasmic
208 replication of a poxvirus and a recent report that Selinexor inhibits SARS-CoV-2 replication, we
209 first tested the effect of Selinexor on the replication of a mouse coronavirus MHV using murine L2
210 cells. To our surprise, we observed that pretreatment of L2 cells with concentrations of Selinexor
211 that had minimal or no toxicity to the cells significantly increased the reporter GFP expression
212 from a recombinant MHV. Furthermore, when we titrated the virus from the infected cells, we also
213 observed increased progeny virus production in the L2 cells. Since our previous observation with
214 MYXV used human cell lines, we tested whether Selinexor similarly affects MHV in human cells.
215 Human HeLa and A549 cells expressing the MHV receptor murine CECAM1 were used (30).
216 Again, increased GFP expression and MHV replication were observed when cells were pretreated
217 with Selinexor concentrations that had minimal or no effect on the cell viability. These results
218 confirm that the impact of Selinexor on MHV replication is independent of the cell type.

219 Since XPO1 is the only known cellular target of Selinexor, we previously reported that XPO1
220 knockdown using siRNA enhanced the replication of MYXV in human cancer cells (26). Here, we
221 used the same approach to confirm that the Selinexor-mediated enhancement of MHV replication
222 is through XPO1/CRM1. Using siRNA, we transiently knocked down XPO1 in both A549-MHVR
223 and HeLa-MHVR cell lines. Under these conditions, we again observed a significant increase in
224 GFP expression and MHV replication when infected at low MOI. These results encouraged us to
225 test whether the optimized lower concentration of Selinexor enhances SARS-COV-2 replication
226 in human cells. In this case, we used A549 cells expressing the SARS-CoV-2 ACE2 receptor.
227 Using a recombinant SARS-CoV-2 that expresses GFP, we show that with a Selinexor
228 concentration of 0.01 μM, there is an increase in GFP expression, which also correlated with
229 increased virus titer. These results indicate that in human cells, both MHV and SARS-CoV-2
230 replication is enhanced by Selinexor treatment. In a recent study, it was shown that in Vero E6
231 cells, Selinexor treatment reduced the SARS-CoV-2 plaque number and virus titer by more than
232 two logs with >10nM Selinexor (24). However, on our hand, Selinexor-mediated enhancement of
233 virus replication was not observed in Vero-E6 cells (data not shown). This is consistent with our
234 observation that MYXV replication is also not enhanced by Selinexor in Vero-E6 cells (data not
235 shown). Therefore, we can speculate that nonhuman primates and human cells respond to
236 Selinexor differently against these tested viruses.

237 To understand the possible mechanisms of how Selinexor enhances coronavirus replication, we
238 studied the localization of RNA helicase DHX9 in the MHV-infected human cells. DHX9 is primarily
239 localized in the nucleus. However, due to its involvement with diverse cellular processes such as
240 transcription and translation, it shuttles between the nuclear and cytosolic compartments. We
241 reported that in the MYXV-infected human cancer cells, DHX9 was exported from the nucleus to
242 form the antiviral granules in the cytoplasm of infected human cancer cells (33). These antiviral
243 granules reduced virus late protein synthesis and reduced progeny virus formation. DHX9 is

244 associated with the replication of many RNA and DNA viruses such as human immunodeficiency
245 virus HIV-1 (39), hepatitis C Virus (40), influenza A (41), hepatitis E (42), cytomegalovirus (43),
246 chikungunya virus (44, 45). In the case of MHV, we observed that in the infected cells, the majority
247 of DHX9 remains still localized in the nucleus; additionally, DHX9 also accumulated in the
248 perinuclear region of the infected cell cytoplasm. When cells were pretreated with Selinexor,
249 localization of DHX9 in the cytoplasm of infected cells was not observed. Selinexor treatment also
250 enhanced the viral GFP expression compared to the MHV infection alone. This localization of
251 DHX9 in MHV infected cells is different from the distinct antiviral granules observed with MYXV
252 (33). This could be due to the differences in how these two classes of viruses replicate in the
253 cytoplasm. Additionally, direct knockdown of DHX9 using siRNA in human cells didn't significantly
254 enhance MHV replication (data not shown), suggesting that other cellular proteins might be
255 involved in this process. For the majority of RNA viruses that have been tested, DHX9 is known
256 as the cellular factor required for optimum virus replication (46). However, our results indicate that
257 DHX9, at least in these cells, is not needed for coronavirus replication; rather, it has an antiviral
258 role in this case. In future the role of DHX9 in coronavirus replication must be further explored.
259 Several SARS-CoV proteins such as ORF3b, ORF9b and nucleocapsid have been reported to be
260 localize in the nucleus and use the XPO1-mediated export pathway (47). However, a direct impact
261 on virus infection and replication has not been reported. Here, we show that inhibition of XPO1
262 with Selinexor or direct knockdown of XPO1 enhances the gene expression and replication of
263 mouse hepatitis coronavirus and SARS-CoV-2.

264 Selinexor is currently approved for treating selected hematological malignancies such as multiple
265 myeloma and diffuse large B-cell lymphoma (11, 48). Multiple clinical trials are presently
266 undergoing to use Selinexor as a monotherapy or in combination with other treatments against
267 diverse types of malignancies (49, 50). A Phase 2 placebo-controlled trial of oral Selinexor in
268 COVID-19 patients did not show significant differences in clinical outcomes (NCT04349098).

269 Although one published report suggests that Selinexor reduces replication of SARS-CoV-2 and
270 symptoms in animal models, our results indicate that Selinexor enhances replication of both MHV
271 and SARS-CoV-2. Future studies should focus on how Selinexor and nuclear transportation
272 pathway regulate the replication of coronavirus.

273 **Materials and methods**

274 **Cell lines**

275 L2 murine fibroblast cell line and African green monkey kidney Vero cells E6 (obtained from
276 ATCC) were cultured and maintained using Dulbecco's modified Eagle's medium (DMEM)
277 supplemented with 10% FBS, 100 U/ml of penicillin, and 100 µg/ml streptomycin. HeLa-MHVR
278 cell line (human HeLa cell line expressing mouse coronavirus receptor mCECAM1) was provided
279 by Tom Gallagher at Loyola University and maintained using DMEM media with 10% FBS,
280 HEPES buffer, 100 U/ml of penicillin, 100 µg/ml streptomycin, MEM non-essential amino acids,
281 and sodium pyruvate. A549-MHVR (human A549 cell line expressing mouse coronavirus receptor
282 mCECAM1) and $A549^{ACE2}$ (human A549 cell line expressing ACE2 receptor) was provided by
283 Susan Weiss at the Perelman School of Medicine at the University of Pennsylvania and
284 maintained with RPMI1640 media supplemented with 10% FBS, 100 U/ml of penicillin, and 100
285 µg/ml streptomycin (31).

286 **Viruses and viral replication assay**

287 Mouse hepatitis coronavirus MHV A59 that expresses GFP was used for all the assays.
288 rA59/$S_{MHV-2}$-EGFP is a recombinant MHV A59 virus that expresses the spike of MHV-2 in place
289 of the WT protein and GFP (27-29). MHVE-GFP was constructed using a MHV A59 reverse
290 genetics system essentially as previously described (51-54). The coding sequence for the MHV
291 envelope (E) protein was fused to the GFP gene with an intervening tetra glycine linker. The
292 construct was cloned into ORF 4a/b in the G subclone of the MHV infectious clone using SbfI and

293 EcoRV restriction sites. The construct was designed to maintain the transcription regulatory
294 sequences for both ORF 4 and ORF5. Virus was recovered after assembling the full-length
295 genomic cDNA and transcription of full-length genomic RNA as previously described (51-54).
296 Following electroporation into baby hamster kidney grown in 17Cl1 mouse cells virus was
297 recovered and passage 1 stock was grown in mouse 17Cl1 cells and titered in L2 cells by
298 plaque assay. The SARS-CoV-2-GFP virus was provided by Ralph Baric at the University of
299 North Carolina Chapel Hill (32).

300 Viral titers in different cell lines were determined using a viral replication assay. The cells were
301 seeded in 24 well plate ($2x10^5$ cells/well). The next day, the cells were treated for 1h with different
302 concentrations of Selinexor diluted in the appropriate media used for growth of the specific cell
303 lines. Virus was added to the cells (volume calculated based on different multiplicities of infection
304 and incubated for 1h at 37$^o$C in the presence of Selinexor. After 1h, the unbound virus was
305 removed, cells were washed with DPBS (Dulbecco's phosphate-buffered saline) and media
306 without Selinexor was added for further incubation. Both cells and media were collected at
307 different time points and stored at -80°C freezer until processing. Samples were subjected to three
308 freeze/thaw cycles before titration. Afterwards, different dilutions were prepared in the appropriate
309 media and plated on cell lines and fluorescent foci were counted after 24h using a fluorescent
310 microscope. All assays and dilutions were performed in triplicate. For SARS-CoV-2, all infections
311 and virus manipulations were conducted at biosafety level 3 (BSL-3) in the Biodesign Institute
312 using appropriate and IBC-approved personal protective equipment and protocols. For plaque
313 assay, samples were serially diluted 10-fold and absorbed on Vero cells at 37$^o$C for 1h. Cells were
314 overlaid with media plus 0.7% agarose and incubated for two days at 37$^o$C. Cells were fixed with
315 4% paraformaldehyde and subsequently stained with 1% crystal violet for counting the plaques.

316 **Reagents and Antibodies**

317 Rabbit polyclonal antibodies for DHX9 and XPO1 and mouse monoclonal antibody against β-
318 actin were purchased from Thermo Fisher Scientific. HRP-conjugated goat anti-rabbit and anti-
319 mouse IgG antibodies were purchased from Jackson Immuno Research Laboratories. All the
320 secondary antibodies conjugated to Alexa Fluor 488, 594, 568 and 647 were purchased from
321 Thermo Fisher Scientific. Selinexor (KPT330) was purchased from Apex Bio (Tokyo, Japan).

322 **Immunofluorescence**

323 Cells ($5x10^5$-$1x10^6$/dish) were seeded onto glass bottom 35 mm petri dishes overnight. The next
324 day cells were treated with Selinexor or mock treated and infected with the virus. At the indicated
325 time points after treatment cells were washed with PBS three times, fixed with 2%
326 paraformaldehyde in PBS for 12 min at room temperature, washed with PBS three times, and
327 permeabilized in 0.1% Triton X-100 in PBS for 90 sec at room temperature. Fixed cells were
328 washed with PBS 3 times and then blocked with 3% BSA in PBS for 30 min at 37$^o$C °C. Samples
329 were then incubated with primary antibody (1:300 dilution) for 30 min at 37$^o$C °C, washed with
330 PBS six times, and incubated with secondary antibodies conjugated to different Alexa Fluors.
331 After washing again with PBS six times, samples were mounted on glass slides with Vecta Shield
332 (Vectorlabs) containing DAPI (4′,6-diamidino-2-phenylindole) to stain DNA in the nuclei and viral
333 factory. Fluorescence images were captured using confocal microscopy.

334 **siRNA transfection**

335 ON-TARGETplus SMART pool siRNAs for exportin 1/XPO1 and a non-targeting control (NT
336 siRNA) were purchased from Dharmacon (Horizon Discovery). In 24 well plate cells were
337 seeded with 40–50% confluence, left overnight for adherence, and then transfected with
338 siRNAs (40 nM) using Lipofectamine RNAiMAX (Invitrogen) transfection reagent. After 48 h of
339 transfection, the cells were infected with different MOIs of virus for 1h, washed to remove the
340 unbound virus, and incubated with complete media. At the indicated time points, cells were

341 either observed by fluorescence microscopy to monitor and record the expression of
342 fluorescent proteins or harvested and processed for titration of progeny virions. For detection
343 of proteins, Western blot analysis was performed from the total proteins as described before
344 (55).

345 **Cell viability assay**

346 To assess the viability of different cell lines after Selinexor treatment, 10,000 cells were seeded
347 into each well of a 96-well plate. The next day, cells were treated with different concentrations of
348 Selinexor. A minimum of four to five wells were used for each treatment condition, and untreated
349 cells (mock) served as controls. Cell viability at different time points was assessed using MTS
350 reagents (Promega) according to manufacturer instructions.

351 **Statistical analysis**

352 Statistical analyses were performed using GraphPad Prism software. Values are represented as
353 mean ± SD for at least two or three independent experiments. A paired two-tailed Student's t-test
354 was used to determine the significance between the two groups. *P* values are reported as follows:
355 no significant (ns) $P > 0.05$, * $P < 0.05$, ** $P < 0.01$, *** $P < 0.001$, **** $P < 0.0001$.

356 **Acknowledgements**

357 We thank Tom Gallagher (Loyola University) for the HeLa-MHVR cells; Susan Weiss (Perelman
358 School of Medicine at the University of Pennsylvania) for the A549-MHVR cells, $A549^{ACE2}$ cells
359 and rA59/$S_{MHV-2}$-EGFP virus; Ralph Baric (University of North Carolina at Chapel Hill) for the
360 SARS-CoV-2-GFP virus; Efrem Lim and Emily Kaelin (Biodesign Institute, Arizona State
361 University) for performing SARS-CoV-2 qRT-PCR assay.

362 **Funding Statement**

363 This research was supported by grants from the National Institute of Health (NIH) USA (R01
364 AI080607) to G.M. and M.M.R., and a Mercatus Center Fast Grant (G09202-300) to G.M., M.M.R,
365 and B.G.H., NIH R01DK048370-26 Subaward VUMC95054 to B.G.H., Tohono O'Odham Nation
366 Award GR40818 to B.G.H.

367 The funders had no role in the study design, data collection and interpretation, or decision to
368 submit the work for publication.

369 **Figure Legends**

370 Figure 1: Selinexor enhances the replication of MHV in L2 cells. A) Effect of Selinexor on L2 cells
371 viability. Cells were plated in 96 well plate and treated with different concentration of Selinexor
372 and cell viability was measured after 48h. B-D) Effect of Selinexor on MHV virus gene expression
373 and replication. Cells were plated in 24 well plates, treated with the indicated concentration of
374 Selinexor for 1h and infected with rA59/$S_{MHV-2}$-EGFP or MHVE-GFP virus with a MOI of 0.01. B)
375 Fluorescence images were taken 24h post infection with rA59/$S_{MHV-2}$-EGFP; C) percent of GFP
376 positive cells were counted using Countess II cell counter at different time points after infection
377 with rA59/$S_{MHV-2}$-EGFP; D) MHVE-GFP virus replication was measured by plaque assay from the
378 total number of viruses in the cells and supernatant 24h post infection.

379 Figure 2: Selinexor enhances the replication of MHV in human HeLa-MHVR cells. A) Effect of
380 Selinexor on the viability of HeLa-MHVR cells. Cells were plated in 96 well plate and treated with
381 different concentration of Selinexor and cell viability was measured after 48h. B-D) Effect of
382 Selinexor on MHV virus replication in HeLa-MHVR cells. Cells were plated in 24 well plates,
383 treated with indicated concentration of Selinexor for 1h and infected with rA59/$S_{MHV-2}$-EGFP or
384 MHVE-GFP virus with a MOI of 0.01. B) Fluorescence images were taken 24h post infection with
385 rA59/$S_{MHV-2}$-EGFP; C) percent of GFP positive cells at 24h and 48h post infection with rA59/$S_{MHV-}$

386 $_2$-EGFP were counted using Countess II cell counter; D) Total number of viruses in the cells and
387 supernatant was determined by plaque assay 24h post infection of cells with MHVE-GFP.

388 Figure 3: Selinexor enhances the replication of MHV in human A549-MHVR cells. A) Effect of
389 Selinexor on the viability of A549-MHVR cells. Cells were plated in 96 well plate and treated with
390 different concentration of Selinexor and cell viability was measured after 48h. B-C) Effect of
391 Selinexor on MHV virus replication in A549-MHVR cells. Cells were plated in 24 well plates,
392 treated with indicated concentration of Selinexor for 1h and infected with rA59/$S_{MHV-2}$-EGFP or
393 MHVE-GFP virus with a MOI of 0.01. B) percent of GFP positive cells at 24h and 48h post infection
394 with rA59/$S_{MHV-2}$-EGFP were counted using Countess II cell counter; C) Total number of viruses
395 in the cells and supernatant was determined by plaque assay 24h post infection of cells with
396 MHVE-GFP.

397 Figure 4: XPO1 knock down enhances the replication of MHV in human A549-CECAM cells. Cells
398 were plated in 24 well plate, transfected with control non-targeting siRNA (NT-siRNA) or XPO1
399 siRNA for 48h and infected with rA59/$S_{MHV-2}$-EGFP or MHVE-GFP for another 24h. A) Images
400 were taken using a fluorescence microscope 24h post infection with MHVE-GFP; B) Knock down
401 of XPO1 was confirmed with Western blot analysis using anti-XPO1 antibody. Actin was used as
402 total protein loading control. C) percent of GFP positive cells after infection with rA59/$S_{MHV-2}$-EGFP
403 were counted using Countess II cell counter. D) Total number of viruses in the cells and
404 supernatant was determined by plaque assay 24h post infection of cells with MHVE-GFP.

405 Figure 5: Selinexor enhances the replication of SARS-CoV-2 in human $A549^{ACE2}$ cells. Cells were
406 plated in 12 well plates, treated with indicated concentration of Selinexor for 1h and infected with
407 SARS-CoV-2 virus. A) percent of GFP positive cells were counted using Countess II cell counter
408 after fixation of cells. B) Total number of progeny virus formation was measured by plaque assay
409 using Vero E6 cells.

410 Figure 6: Selinexor blocks the cytoplasmic localization of DHX9 in the MHV infected cell. A) HeLa-
411 MHVR cells were seeded on glass bottom 35mm petri dishes and left over-night to adhere. Next
412 day cells were mock infected or infected with rA59/$S_{MHV-2}$-EGFP (MOI = 0.01) in the presence or
413 absence of selinexor. After 24h cells were fixed and stained with antibodies against DHX9. Nuclei
414 were stained with DAPI. B) Titration of progeny virus in the infected cells and supernatant. Cells
415 were plated in 24 well plates, treated with indicated concentration of selinexor for 1h and infected
416 with MHVE-GFP virus with a MOI of 0.1. 24h post infection the cells and supernatants were
417 collected separately. Number of viruses in the cells and supernatants were measured by plaque
418 assay.

419 References:


420 1. Wing CE, Fung HYJ, Chook YM. 2022. Karyopherin-mediated nucleocytoplasmic
421 transport. Nat Rev Mol Cell Biol 23:307-328.
422 2. Tetenbaum-Novatt J, Rout MP. 2010. The mechanism of nucleocytoplasmic transport
423 through the nuclear pore complex. Cold Spring Harb Symp Quant Biol 75:567-84.
424 3. Kumar AV, Kang T, Thakurta TG, Ng C, Rogers AN, Larsen MR, Lapierre LR. 2022.
425 Exportin 1 modulates life span by regulating nucleolar dynamics via the autophagy protein
426 LGG-1/GABARAP. Sci Adv 8:eabj1604.
427 4. Ishikawa C, Mori N. 2022. Exportin-1 is critical for cell proliferation and survival in adult T
428 cell leukemia. Invest New Drugs 40:718-727.
429 5. Azmi AS, Uddin MH, Mohammad RM. 2021. The nuclear export protein XPO1 - from
430 biology to targeted therapy. Nat Rev Clin Oncol 18:152-169.
431 6. Uddin MH, Zonder JA, Azmi AS. 2020. Exportin 1 inhibition as antiviral therapy. Drug
432 Discov Today 25:1775-1781.
433 7. Azizian NG, Li Y. 2020. XPO1-dependent nuclear export as a target for cancer therapy. J
434 Hematol Oncol 13:61.

435 8. Zhao L, Luo B, Wang L, Chen W, Jiang M, Zhang N. 2021. Pan-cancer analysis reveals
436 the roles of XPO1 in predicting prognosis and tumorigenesis. Transl Cancer Res 10:4664-
437 4679.
438 9. Jans DA, Martin AJ, Wagstaff KM. 2019. Inhibitors of nuclear transport. Curr Opin Cell
439 Biol 58:50-60.
440 10. Gerecitano J. 2014. SINE (selective inhibitor of nuclear export)--translational science in a
441 new class of anti-cancer agents. J Hematol Oncol 7:67.
442 11. Goldsmith SR, Liu L, Shiah K. 2022. Selinexor therapy for multiple myeloma and non-
443 Hodgkin lymphomas. Curr Opin Oncol 34:524-530.
444 12. Lassman AB, Wen PY, van den Bent MJ, Plotkin SR, Walenkamp AME, Green AL, Li K,
445 Walker CJ, Chang H, Tamir S, Henegar L, Shen Y, Alvarez MJ, Califano A, Landesman
446 Y, Kauffman MG, Shacham S, Mau-Sørensen M. 2022. A Phase II Study of the Efficacy
447 and Safety of Oral Selinexor in Recurrent Glioblastoma. Clin Cancer Res 28:452-460.
448 13. Pickens JA, Tripp RA. 2018. Verdinexor Targeting of CRM1 is a Promising Therapeutic
449 Approach against RSV and Influenza Viruses. Viruses 10.
450 14. Sajidah ES, Lim K, Wong RW. 2021. How SARS-CoV-2 and Other Viruses Build an
451 Invasion Route to Hijack the Host Nucleocytoplasmic Trafficking System. Cells 10.
452 15. Paules CI, Marston HD, Fauci AS. 2020. Coronavirus Infections-More Than Just the
453 Common Cold. Jama 323:707-708.
454 16. V'Kovski P, Kratzel A, Steiner S, Stalder H, Thiel V. 2021. Coronavirus biology and
455 replication: implications for SARS-CoV-2. Nat Rev Microbiol 19:155-170.
456 17. Fung TS, Liu DX. 2019. Human Coronavirus: Host-Pathogen Interaction. Annu Rev
457 Microbiol 73:529-557.
458 18. Zhang T, Wu Q, Zhang Z. 2020. Probable Pangolin Origin of SARS-CoV-2 Associated
459 with the COVID-19 Outbreak. Curr Biol 30:1346-1351.e2.

460 19. Mahilkar S, Agrawal S, Chaudhary S, Parikh S, Sonkar SC, Verma DK, Chitalia V, Mehta
461 D, Koner BC, Vijay N, Shastri J, Sunil S. 2022. SARS-CoV-2 variants: Impact on biological
462 and clinical outcome. Front Med (Lausanne) 9:995960.
463 20. Wiegand T, Nemudryi A, Nemudraia A, McVey A, Little A, Taylor DN, Walk ST, Wiedenheft
464 B. 2022. The Rise and Fall of SARS-CoV-2 Variants and Ongoing Diversification of
465 Omicron. Viruses 14.
466 21. Madden EA, Diamond MS. 2022. Host cell-intrinsic innate immune recognition of SARS-
467 CoV-2. Curr Opin Virol 52:30-38.
468 22. Lv L, Zhang L. 2021. Host proviral and antiviral factors for SARS-CoV-2. Virus Genes
469 57:475-488.
470 23. Baggen J, Vanstreels E, Jansen S, Daelemans D. 2021. Cellular host factors for SARS-
471 CoV-2 infection. Nat Microbiol 6:1219-1232.
472 24. Kashyap T, Murray J, Walker CJ, Chang H, Tamir S, Hou B, Shacham S, Kauffman MG,
473 Tripp RA, Landesman Y. 2021. Selinexor, a novel selective inhibitor of nuclear export,
474 reduces SARS-CoV-2 infection and protects the respiratory system in vivo. Antiviral Res
475 192:105115.
476 25. Mostafa-Hedeab G, Al-Kuraishy HM, Al-Gareeb AI, Welson NN, El-Saber Batiha G,
477 Conte-Junior CA. 2022. Selinexor and COVID-19: The Neglected Warden. Front
478 Pharmacol 13:884228.
479 26. Rahman MM, Oosterom F, Enow JA, Hossain M, Gutierrez-Jensen A, Cashen M, Everts
480 A, Lowe K, Kilbourne J, Daggett-Vondras J, Karr TL, McFadden G. 2022. A novel anti-
481 cancer therapy with nuclear export inhibitor Selinexor in combination with oncolytic
482 myxoma virus. bioRxiv doi:10.1101/2022.10.31.514585.
483 27. Das Sarma J, Fu L, Tsai JC, Weiss SR, Lavi E. 2000. Demyelination determinants map to
484 the spike glycoprotein gene of coronavirus mouse hepatitis virus. J Virol 74:9206-13.

485 28. Das Sarma J, Iacono K, Gard L, Marek R, Kenyon LC, Koval M, Weiss SR. 2008.
486 Demyelinating and nondemyelinating strains of mouse hepatitis virus differ in their neural
487 cell tropism. J Virol 82:5519-26.
488 29. Qiu Z, Hingley ST, Simmons G, Yu C, Das Sarma J, Bates P, Weiss SR. 2006. Endosomal
489 proteolysis by cathepsins is necessary for murine coronavirus mouse hepatitis virus type
490 2 spike-mediated entry. J Virol 80:5768-76.
491 30. Rao PV, Gallagher TM. 1998. Intracellular complexes of viral spike and cellular receptor
492 accumulate during cytopathic murine coronavirus infections. J Virol 72:3278-88.
493 31. Li Y, Renner DM, Comar CE, Whelan JN, Reyes HM, Cardenas-Diaz FL, Truitt R, Tan LH,
494 Dong B, Alysandratos KD, Huang J, Palmer JN, Adappa ND, Kohanski MA, Kotton DN,
495 Silverman RH, Yang W, Morrisey EE, Cohen NA, Weiss SR. 2021. SARS-CoV-2 induces
496 double-stranded RNA-mediated innate immune responses in respiratory epithelial-derived
497 cells and cardiomyocytes. Proc Natl Acad Sci U S A 118.
498 32. Hou YJ, Okuda K, Edwards CE, Martinez DR, Asakura T, Dinnon KH, 3rd, Kato T, Lee
499 RE, Yount BL, Mascenik TM, Chen G, Olivier KN, Ghio A, Tse LV, Leist SR, Gralinski LE,
500 Schäfer A, Dang H, Gilmore R, Nakano S, Sun L, Fulcher ML, Livraghi-Butrico A, Nicely
501 NI, Cameron M, Cameron C, Kelvin DJ, de Silva A, Margolis DM, Markmann A, Bartelt L,
502 Zumwalt R, Martinez FJ, Salvatore SP, Borczuk A, Tata PR, Sontake V, Kimple A, Jaspers
503 I, O'Neal WK, Randell SH, Boucher RC, Baric RS. 2020. SARS-CoV-2 Reverse Genetics
504 Reveals a Variable Infection Gradient in the Respiratory Tract. Cell 182:429-446.e14.
505 33. Rahman MM, Gutierrez-Jensen AD, Glenn HL, Abrantes M, Moussatche N, McFadden G.
506 2021. RNA Helicase A/DHX9 Forms Unique Cytoplasmic Antiviral Granules That Restrict
507 Oncolytic Myxoma Virus Replication in Human Cancer Cells. J Virol 95:e0015121.
508 34. Mathew C, Ghildyal R. 2017. CRM1 Inhibitors for Antiviral Therapy. Front Microbiol
509 8:1171.

510 35. Ferreira BI, Cautain B, Grenho I, Link W. 2020. Small Molecule Inhibitors of CRM1. Front
511 Pharmacol 11:625.
512 36. Newlands ES, Rustin GJ, Brampton MH. 1996. Phase I trial of elactocin. Br J Cancer
513 74:648-9.
514 37. Perwitasari O, Johnson S, Yan X, Howerth E, Shacham S, Landesman Y, Baloglu E,
515 McCauley D, Tamir S, Tompkins SM, Tripp RA. 2014. Verdinexor, a novel selective
516 inhibitor of nuclear export, reduces influenza a virus replication in vitro and in vivo. J Virol
517 88:10228-43.
518 38. Mathew C, Tamir S, Tripp RA, Ghildyal R. 2021. Reversible disruption of XPO1-mediated
519 nuclear export inhibits respiratory syncytial virus (RSV) replication. Sci Rep 11:19223.
520 39. Brady S, Singh G, Bolinger C, Song Z, Boeras I, Weng K, Trent B, Brown WC, Singh K,
521 Boris-Lawrie K, Heng X. 2019. Virion-associated, host-derived DHX9/RNA helicase A
522 enhances the processivity of HIV-1 reverse transcriptase on genomic RNA. J Biol Chem
523 294:11473-11485.
524 40. He QS, Tang H, Zhang J, Truong K, Wong-Staal F, Zhou D. 2008. Comparisons of RNAi
525 approaches for validation of human RNA helicase A as an essential factor in hepatitis C
526 virus replication. J Virol Methods 154:216-9.
527 41. Lin L, Li Y, Pyo HM, Lu X, Raman SN, Liu Q, Brown EG, Zhou Y. 2012. Identification of
528 RNA helicase A as a cellular factor that interacts with influenza A virus NS1 protein and
529 its role in the virus life cycle. J Virol 86:1942-54.
530 42. Paingankar MS, Arankalle VA. 2015. Identification and characterization of cellular proteins
531 interacting with Hepatitis E virus untranslated regions. Virus Res 208:98-109.
532 43. Lenarcic EM, Ziehr BJ, Moorman NJ. 2015. An unbiased proteomics approach to identify
533 human cytomegalovirus RNA-associated proteins. Virology 481:13-23.
534 44. Matkovic R, Bernard E, Fontanel S, Eldin P, Chazal N, Hassan Hersi D, Merits A,
535 Peloponese JM, Jr., Briant L. 2019. The Host DHX9 DExH-Box Helicase Is Recruited to

536 Chikungunya Virus Replication Complexes for Optimal Genomic RNA Translation. J Virol
537 93.
538 45. Guo F, Xing L. 2021. RNA helicase A as co-factor for DNA viruses during replication. Virus
539 Res 291:198206.
540 46. Fullam A, Schroder M. 2013. DExD/H-box RNA helicases as mediators of anti-viral innate
541 immunity and essential host factors for viral replication. Biochim Biophys Acta 1829:854-
542 65.
543 47. Chen M, Ma Y, Chang W. 2022. SARS-CoV-2 and the Nucleus. Int J Biol Sci 18:4731-
544 4743.
545 48. Nachmias B, Schimmer AD. 2020. Targeting nuclear import and export in hematological
546 malignancies. Leukemia 34:2875-2886.
547 49. Landes JR, Moore SA, Bartley BR, Doan HQ, Rady PL, Tyring SK. 2022. The efficacy of
548 selinexor (KPT-330), an XPO1 inhibitor, on non-hematologic cancers: a comprehensive
549 review. J Cancer Res Clin Oncol doi:10.1007/s00432-022-04247-z.
550 50. Galinski B, Alexander TB, Mitchell DA, Chatwin HV, Awah C, Green AL, Weiser DA. 2021.
551 Therapeutic Targeting of Exportin-1 in Childhood Cancer. Cancers (Basel) 13.
552 51. Verma S, Lopez LA, Bednar V, Hogue BG. 2007. Importance of the penultimate positive
553 charge in mouse hepatitis coronavirus A59 membrane protein. JVirol 81:5339-5348.
554 52. Ye Y, Hogue BG. 2007. Role of the coronavirus E viroporin protein transmembrane
555 domain in virus assembly. JVirol 81:3597-3607.
556 53. Lopez LA, Riffle AJ, Pike SL, Gardner D, Hogue BG. 2008. Importance of conserved
557 cysteine residues in the coronavirus envelope protein. JVirol 82:3000-3010.
558 54. Arndt AL, Larson BJ, Hogue BG. 2010. A conserved domain in the coronavirus membrane
559 protein tail is important for virus assembly. JVirol 84:11418-11428.

560 55. Rahman MM, Bagdassarian E, Ali MAM, McFadden G. 2017. Identification of host DEAD-
561 box RNA helicases that regulate cellular tropism of oncolytic Myxoma virus in human
562 cancer cells. Sci Rep 7:15710.

563

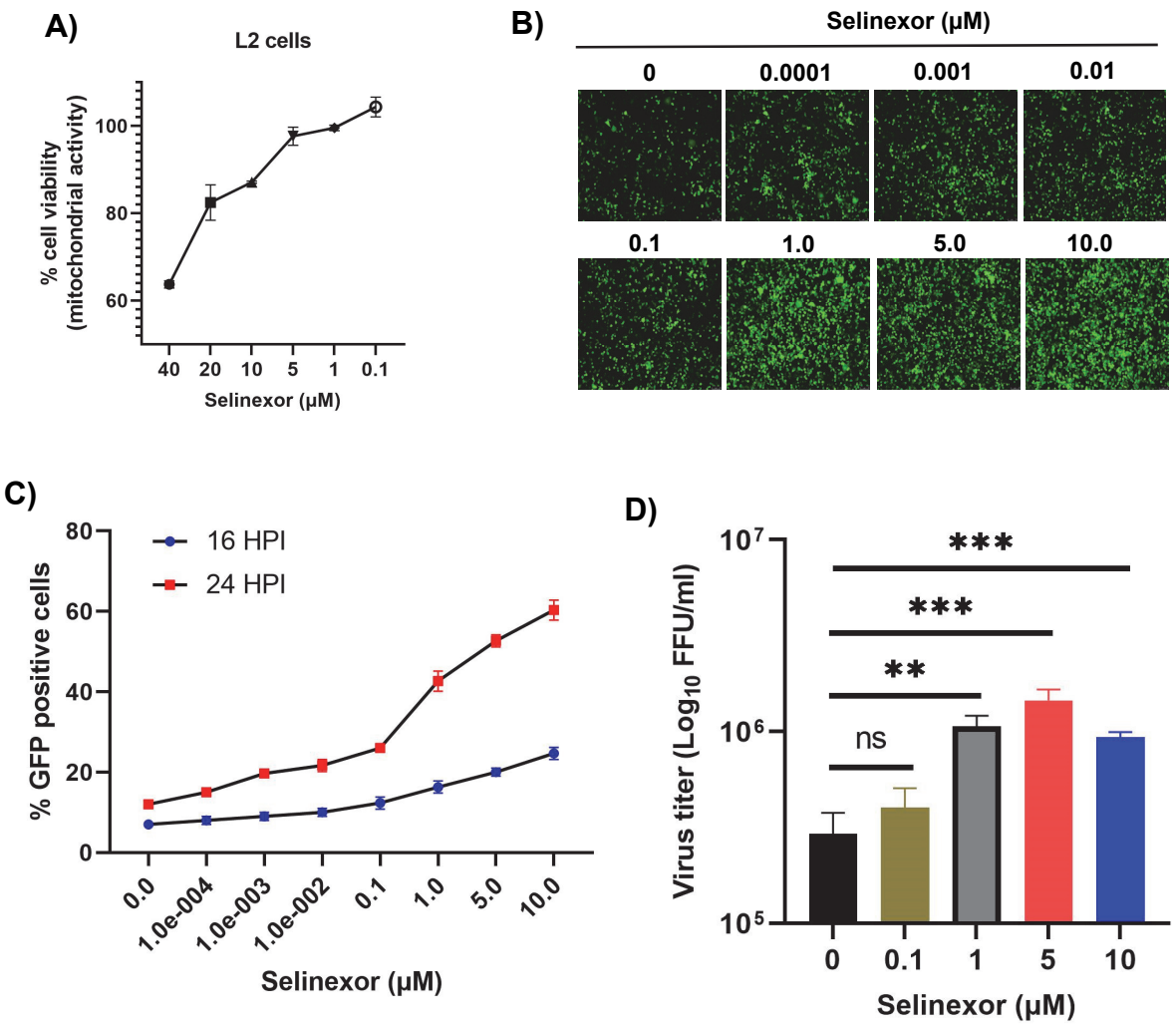


Figure 1: Selinexor enhances the replication of MHV in L2 cells. A) Effect of Selinexor on L2 cells viability. Cells were plated in 96 well plate and treated with different concentration of Selinexor and cell viability was measured after 48h. B-D) Effect of Selinexor on MHV virus gene expression and replication. Cells were plated in 24 well plates, treated with the indicated concentration of Selinexor for 1h and infected with rA59/$S_{MHV-2}$-EGFP or MHVE-GFP virus with a MOI of 0.01. B) Fluorescence images were taken 24h post infection with rA59/$S_{MHV-2}$-EGFP; C) percent of GFP positive cells were counted using Countess II cell counter at different time points after infection with rA59/$S_{MHV-2}$-EGFP; D) MHVE-GFP virus replication was measured by plaque assay from the total number of viruses in the cells and supernatant 24h post infection.

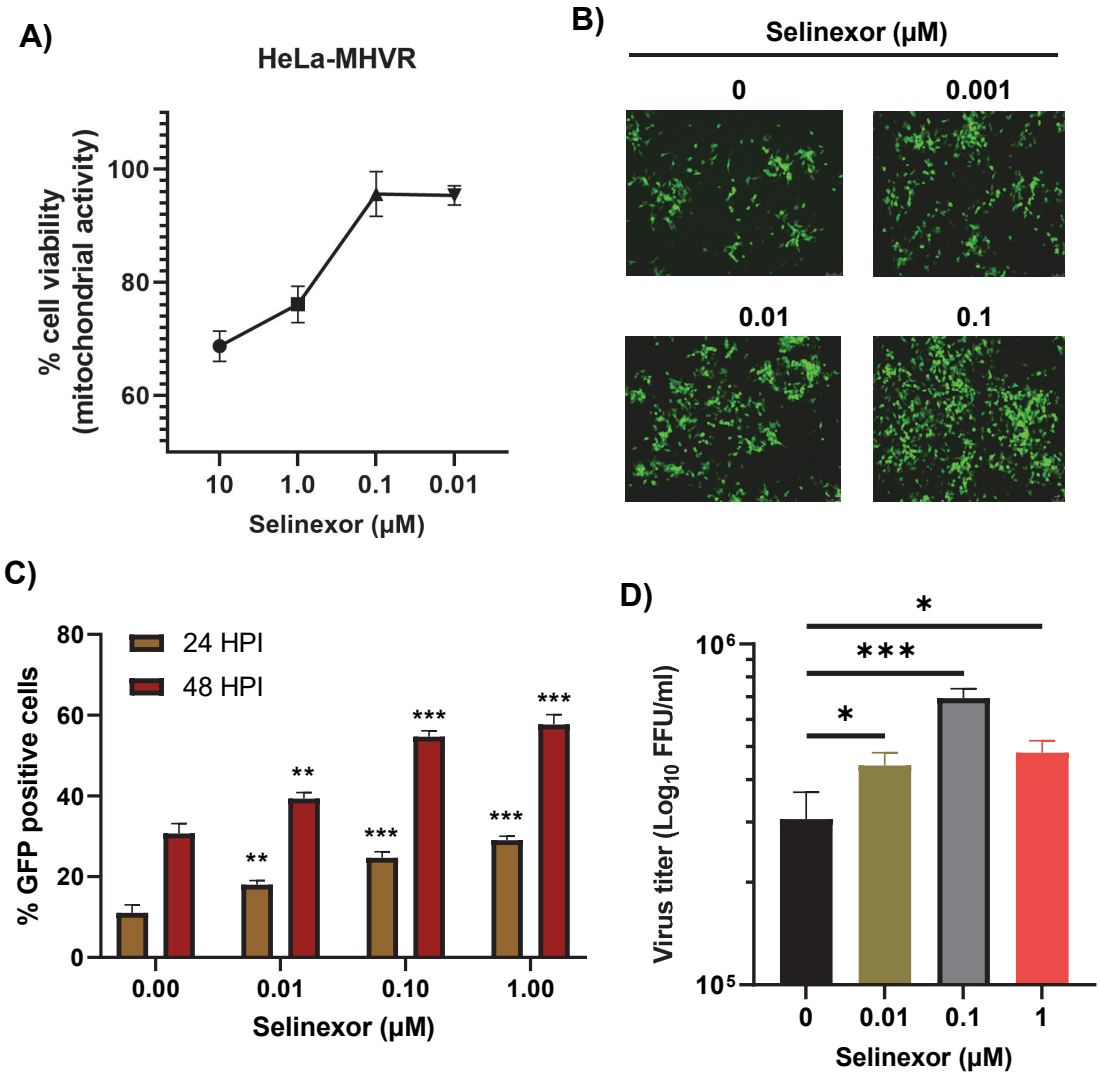


Figure 2: Selinexor enhances the replication of MHV in human HeLa-MHVR cells. A) Effect of Selinexor on the viability of HeLa-MHVR cells. Cells were plated in 96 well plate and treated with different concentration of Selinexor and cell viability was measured after 48h. B-D) Effect of Selinexor on MHV virus replication in HeLa-MHVR cells. Cells were plated in 24 well plates, treated with indicated concentration of Selinexor for 1h and infected with rA59/$S_{MHV-2}$-EGFP or MHVE-GFP virus with a MOI of 0.01. B) Fluorescence images were taken 24h post infection with rA59/$S_{MHV-2}$-EGFP; C) percent of GFP positive cells at 24h and 48h post infection with rA59/$S_{MHV-2}$-EGFP were counted using Countess II cell counter; D) Total number of viruses in the cells and supernatant was determined by plaque assay 24h post infection of cells with MHVE-GFP.

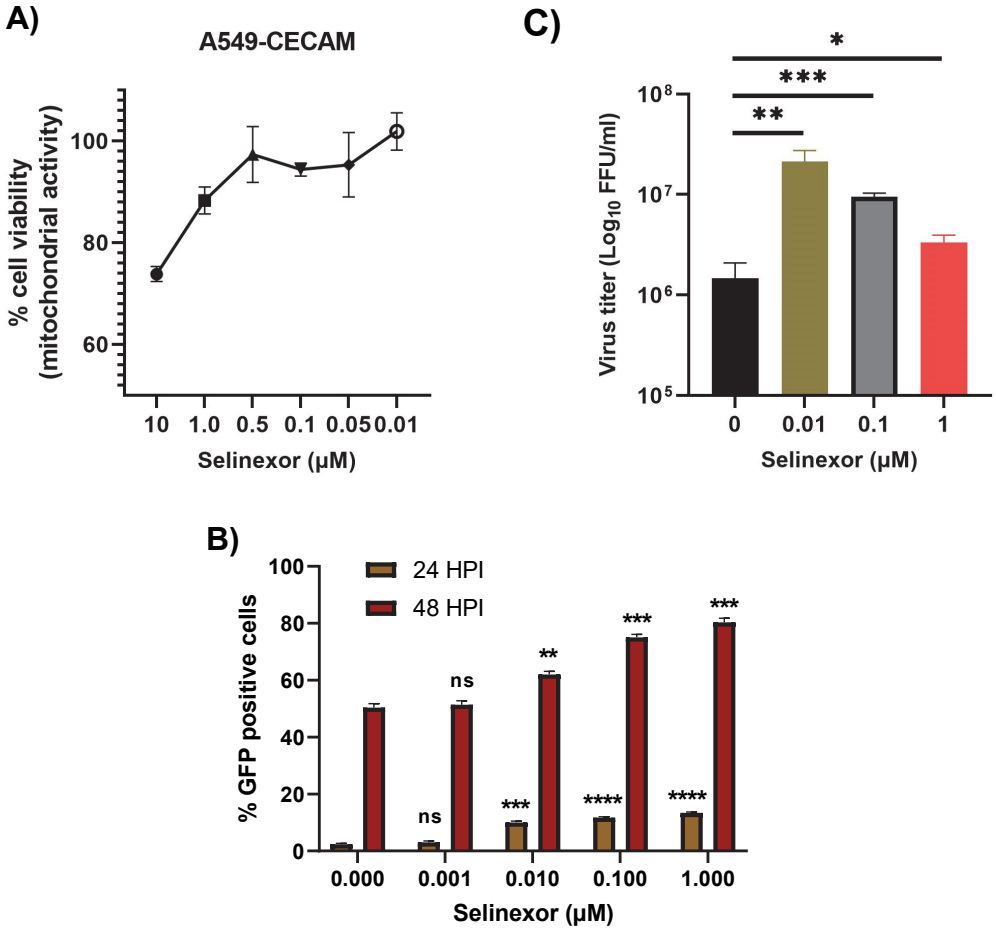


Figure 3: Selinexor enhances the replication of MHV in human A549-MHVR cells. A) Effect of Selinexor on the viability of A549-MHVR cells. Cells were plated in 96 well plate and treated with different concentration of Selinexor and cell viability was measured after 48h. B-C) Effect of Selinexor on MHV virus replication in A549-MHVR cells. Cells were plated in 24 well plates, treated with indicated concentration of Selinexor for 1h and infected with rA59/$S_{MHV-2}$-EGFP or MHVE-GFP virus with a MOI of 0.01. B) percent of GFP positive cells at 24h and 48h post infection with rA59/$S_{MHV-2}$-EGFP were counted using Countess II cell counter; C) Total number of viruses in the cells and supernatant was determined by plaque assay 24h post infection of cells with MHVE-GFP.

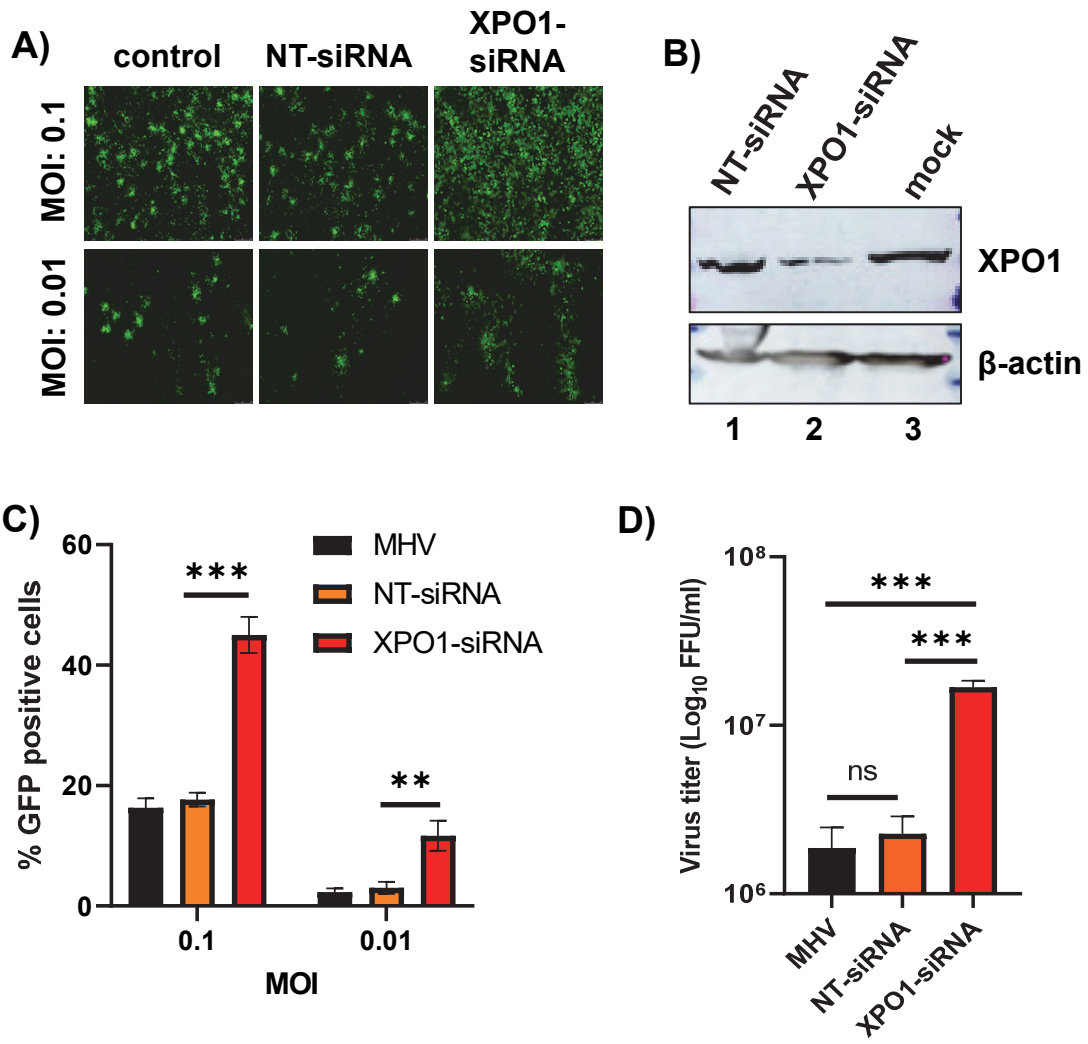


Figure 4: XPO1 knock down enhances the replication of MHV in human A549-CECAM cells. Cells were plated in 24 well plate, transfected with control non-targeting siRNA (NT-siRNA) or XPO1 siRNA for 48h and infected with rA59/$S_{MHV-2}$-EGFP or MHVE-GFP for another 24h. A) Images were taken using a fluorescence microscope 24h post infection with MHVE-GFP; B) Knock down of XPO1 was confirmed with Western blot analysis using anti-XPO1 antibody. Actin was used as total protein loading control. C) percent of GFP positive cells after infection with rA59/$S_{MHV-2}$-EGFP were counted using Countess II cell counter. D) Total number of viruses in the cells and supernatant was determined by plaque assay 24h post infection of cells with MHVE-GFP.

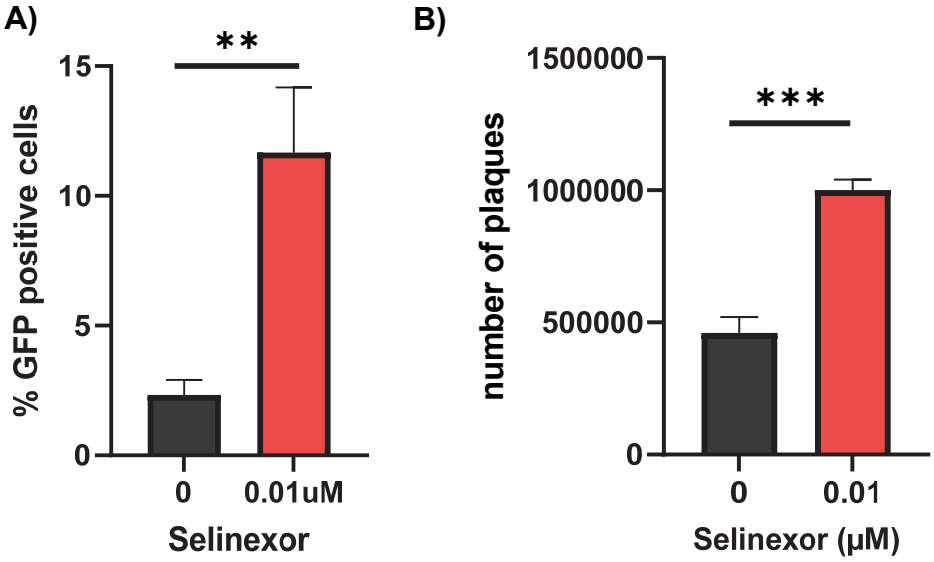


Figure 5: Selinexor enhances the replication of SARS-CoV-2 in human A549$^{ACE2}$ cells. Cells were plated in 12 well plates, treated with indicated concentration of Selinexor for 1h and infected with SARS-CoV-2 virus. A) percent of GFP positive cells were counted using Countess II cell counter after fixation of cells. B) Total number of progeny virus formation was measured by plaque assay using Vero E6 cells.

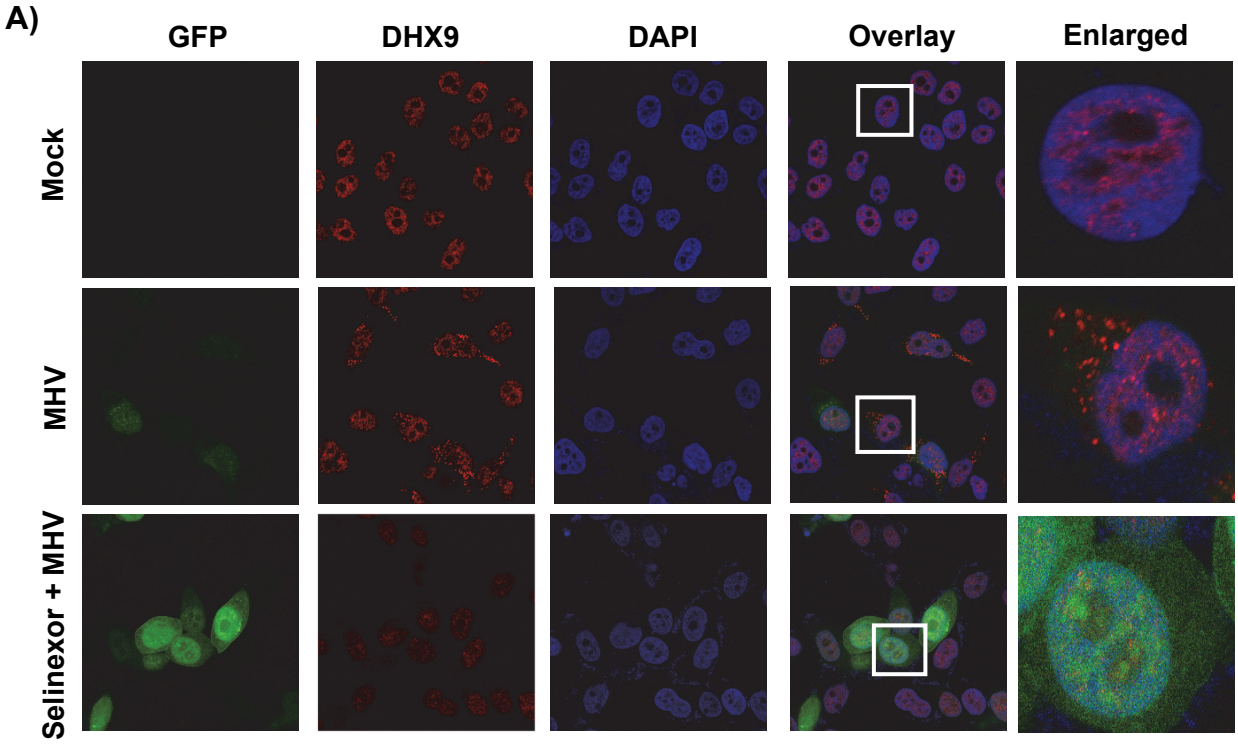


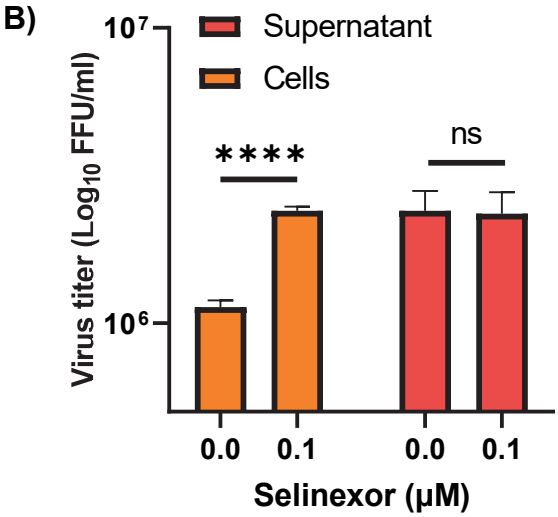


Figure 6: Selinexor blocks the cytoplasmic localization of DHX9 in the MHV infected cell. A) HeLa-MHVR cells were seeded on glass bottom 35mm petri dishes and left over-night to adhere. Next day cells were mock infected or infected with rA59/$S_{MHV-2}$-EGFP (MOI = 0.01) in the presence or absence of selinexor. After 24h cells were fixed and stained with antibodies against DHX9. Nuclei were stained with DAPI. B) Titration of progeny virus in the infected cells and supernatant. Cells were plated in 24 well plates, treated with indicated concentration of selinexor for 1h and infected with MHVE-GFP virus with a MOI of 0.1. 24h post infection the cells and supernatants were collected separately. Number of viruses in the cells and supernatants were measured by plaque assay.